Basic Res Cardiol 96: 539 – 546 (2001)

Mitsuru Momose
Leisha Tyndale-Hines
Frank Michael Bengel
Markus Schwaiger

How heterogeneous is the cardiac autonomic innervation?

Abbreviations

MIBG	=	I-123 metaiodobenzylguanidine
NE	=	norepinephrine
SPECT	=	single photon emission tomography
HED	=	C-11 hydroxyephedrine
PET	=	positron emission tomography
VT	=	ventricular tachycardia
ARVC	=	arrhythmogenic right ventricular cardiomyopathy
ILVT	=	idiopathic left ventricular tachycardia
IVF	=	idiopathic ventricular fibrillation
DCM	=	dilated cardiomyopathy
HCM	=	hypertrophic cardiomyopathy
F-18 FDA	=	F-18 fluorodopamine

Received: 2 April 2001
Returned for revision: 28 June 2001
Revision received: 7 August 2001
Accepted: 31 August 2001

M. Momose, MD. · L. Tyndale-Hines, B.Sc. (Hons) · F. M. Bengel, MD.
M. Schwaiger, M.D. (✉)
Nuklearmedizinische Klinik und Poliklinik der Technischen Universität München
Klinikum rechts der Isar
Ismaninger Straße 22
81675 München, Germany
Tel.: +49-89/4140-2971
Fax: +49-89/4140-4841

Abstract The rich autonomic innervation of the heart plays an important role in modifying cardiovascular function. Recently developed in vivo scintigraphic imaging techniques allow for visualization of the autonomic innervation of the heart. Studies using the modalities have shown heterogeneity of sympathetic innervation in various kinds of pathological conditions as well as normal human heart. The inferioposterior region shows typically less sympathetic innervation than the anterior region. In addition, neuropathic processes appear to commence in inferior-apical regions extending towards the base of the heart. Arrhythmogeneity has been related to the heterogeneous innervation of the heart and heterogeneous uptake of radiolabeled catecholamine analogues, such as I-123 metaiodobenzylguanidine, can be found in patients with arrhythmia. In dilated cardiomyopathy, reduced uptake indicates a poor prognosis which allows risk stratification for patients with heart failure. Heterogeneity of the reinnervation process following heart transplantation has also been investigated. Evidence was found of reinnervation primarily in the basal anterioseptal region and to a lesser degree in the inferioposterior and apical regions. Tracer approaches are uniquely suited to identify regionally altered innervation and provide tools for linking information on cardiac autonomic innervation with other clinical aspects.

Key words Heterogeneity – cardiac sympathetic nerves – I-123 MIBG – C-11 hydroxyephedrine – denervation

Introduction

The rich autonomic innervation of the heart plays an important role in modifying cardiovascular function (38). Numerous articles have addressed cardiovascular

autonomic regulation by the central nervous system and physiological processes. Recently developed in vivo scintigraphic imaging enables the autonomic innervation of the heart to be visualized (35, 54, 66). However the sparse cholinergic innervation of the ventricles limits the presynaptic evaluation of this system in vivo. Therefore, most imaging approaches focus on the scintigraphic delineation of the sympathetic nervous systems because the left and right ventricles are densely innervated by sympathetic fibers. Studies using these modalities have shown heterogeneity of sympathetic innervation in various kinds of pathological conditions (17, 26, 30, 45, 52, 59, 63, 67) as well as the normal human heart (14, 33, 47, 62). As autonomic heterogeneity has been linked to arrhythmias and sudden death, it appears important to study the heterogeneity of the heart (5, 8). Heterogeneity of the reinnervation process following heart transplantation has also been investigated (4, 31, 53) and this together with the above will be discussed in this brief review.

Anatomical and functional autonomic nerve projections to the heart

Autonomic nerve projections into the heart promote understanding of how the autonomic nervous system regulates the heart (Fig. 1). James et al. (19) described the anatomy of cardiac sympathetic nerve projections into the human heart. The right stellate cardiopulmonary nerve, from the right stellate ganglia, courses through the dorsal nerve plexus to the left lateral cardiopulmonary nerve and projects into the lateral wall of the left ventricle. The dorsal medial and lateral cardiopulmonary nerves, from the central cervical ganglia, form the left coronary nerve which runs alongside the main left coronary artery. The coronary artery, in turn, separates into two branches running alongside the circumflex and left anterior descending coronary arteries and on into the adjacent epicardium. The left ventral cardiopulmonary nerve, from the left cervical ganglia, connects solely to the right coronary cardiac nerve which runs adjacent to the right coronary artery and projects into the right ventricle and inferior posterior wall of the left ventricle. The left dorsal cardiopulmonary nerves join with the right dorsal cardiopulmonary nerves to form the dorsal plexus and the left coronary cardiac nerve: a connection also exists between the dorsal plexus and the right coronary cardiac nerve. None of the sympathetic nerve projections, however, influence an exclusive cardiac territory, although the anterior region of the left ventricle appears to be mainly regulated by nerve fibers from the right sympathetic ganglia.

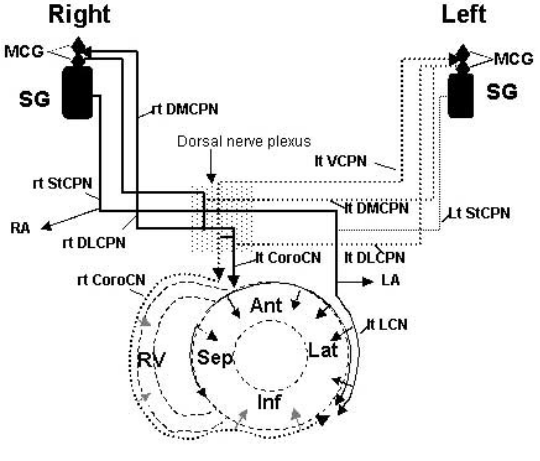

Fig. 1 Cardiac nerve projections to the heart (*MCG* middle cervical ganglia; *SG* stellate ganglia; *rt* right; *lt* left; *StCPN* stellate cardiopulmonary nerve; *VCPN* ventral cardiopulmonary nerve; *DLCPN* dorsal lateral cardiopulmonary nerve; *DMCPN* dorsal medial cardiopulmonary nerve; *CoroCN* coronary cardiac nerve; *LCN* lateral cardiac nerve; *RA* right atria; *LA* left atria). See details in the text.

A number of functional canine heart studies support James et al.'s description (19). Schlock et al. (51) demonstrated how a left stellate ganglion block on canine hearts significantly reduced contractility in the posteriobasal myocardium compared to the anterioapical region. Norepinephrine analogue I-123 metaiodobenzylguanidine (MIBG), used in in vivo imaging studies on canine hearts, revealed an increased uptake in the anterioapical region following a left stellate ganglion block and an increased uptake in the posterior region following a right stellate ganglion block (9).

The parasympathetic innervation of the heart is provided by efferent paraganglionic parasympathetic neurons in the medulla oblongata, which project axons onto the heart where they synapse with efferent postganglionic parasympathetic neurons that innervate the heart. Despite the existence of an abundant parasympathetic innervation of the atria, intraventricular parasympathetic ganglion cells are sparsely distributed (36). Pace et al. (40) reported that reduced contractility was observed more markedly in the left ventricular base than in the apex by stimulation of the cervical vagosympathetic trunk, indicating less innervation in the apex than in the base of the left ventricle.

Thames et al. (60) found that left ventricular receptors with vagal afferents are located mainly in the inferioposterior region. As these receptors are activated during coronary occlusion and mediate cardioinhibitory and vasodepressor responses, this may explain why acute inferioposterior myocardial infarction induces a greater number of negative reflex responses, such as bradycardia, hypotension and vasodilation, than acute inferior infarction. These functional studies support Randall et al.'s (46) descriptions of the "patterns of sympathetic nerve projections onto the canine heart".

In summary, sympathetic nerves distributed in the anterior region are most likely to be regulated by the right sympathetic basal ganglia whereas those in the inferioposterior region are most likely to be regulated by the left sympathetic basal ganglia. Furthermore, the inferioposterior region of the heart contains a greater number of ventricular receptors with parasympathetic vagal afferent nerves than the anterior region. However, in summarizing, possible variations between canine and human hearts should not be forgotten.

Heterogeneous norepinephrine content in the heart

Pierpont et al. (41) investigated the myocardial norepinephrine (NE) content of four healthy dogs. The NE concentration was found to be higher in the atria than in the ventricle with NE distribution in the left ventricle demonstrating a gradient from apex to base. No epicardial-to-endocardial gradient was present. NE uptake ratio in the left ventricle, following radiolabeled NE injection revealed a similar heterogeneous pattern. These results suggest that areas of high tissue NE uptake represent regions rich in adrenergic supply and high in adrenergic activity; therefore, the left ventricular base area appears to be more richly innervated than the apical area.

Heterogeneity in normal human heart

Recent studies using I-123 MIBG scintigraphy have demonstrated the heterogeneous sympathetic distribution of the normal heart (14, 47, 62, 33). Previous investigations on uptake rates immediately following I-123 MIBG injection, seem to reflect the anatomical distribution of sympathetic nerve endings (7, 45), whereas later (4 hour) imaging reflects the functional distribution of the sympathetic system. Furthermore, washout rate from early to late uptake might reflect regional sympathetic tone (3, 18, 25, 30). Tsuchimochi et al. (62) used MIBG to investigate delayed uptake in twenty-nine normal human subjects. They found that only in the inferior region did uptake decrease with age and that this was more evident in men. Sakata et al. (47) investigated regional heterogeneity, focusing on regional functional differences, using 315 normal subjects (40 – 79 years old) assessed by the washout rate of I-123 MIBG. They found, in men, that MIBG uptake at late imaging in the inferior region was inversely correlated to age, with a 16% reduction in uptake in the 80-year-old age group compared to the 40-year-old age group. Furthermore in the female groups, MIBG washout rates in each region: anterior, lateral and inferior were also well correlated with age. The authors stated that the age-related inferior MIBG decreased uptake in men could be explained by impaired re-uptake of norepinephrine. In women, age-related, diffusely enhanced MIBG washout, was believed to be a result of reduced parasympathetic nerve activity. Morozumi et al. (33) reported that inferior MIBG uptake was inversely correlated with the high frequency component, assessed by Holter ECG, as an index of parasympathetic nerve activity and mean R-R interval in resting ECG in normal human subjects. The high parasympathetic activity in patients with low inferior tracer uptake may be caused by the depressor reflex mediated by the parasympathetic nerve fibers, secondary to age-induced neuronal depletion as indicated above (60).

I-123 MIBG imaging was used to study cardiac heterogeneous innervation in structurally normal hearts of athletes with sinus bradycardia (12). A severely depressed inferior uptake of MIBG was found compared to controls ($44 \pm 13\%$ vs. $72 \pm 11\%$, $p < 0.01$) which may also induce high parasympathetic activity, characterized by sinus bradycardia.

The mechanism of sympathetic cardiac innervation has yet to be clarified but, as shown in Fig. 1, inferior, posterior and apical regions are regulated by the terminal portions of the cardiac sympathetic nerves. Length-dependent alterations of the sympathetic nerve density might be one possible explanation of the heterogeneity.

Diaphragmatic attenuation of scintigraphic data sometimes plays a role in the heterogeneity of MIBG distribution in the left ventricle upon imaging, in particular in the inferioposterior region. Furthermore, a previous phantom study demonstrated that a high count in the liver may create artifactual defects in the inferioposterior region of the heart in single photon emission tomography (SPECT) imaging (23). However if age-related lower MIBG uptake rates are considered, these artifacts may contribute less to the heterogeneity of MIBG distribution.

Heterogeneity in arrhythmogenic heart disease

The sympathetic nervous system is known to play an important role in the genesis of ventricular arrhythmias (68). Increased levels of catecholamines or cardiac sympathetic overactivity can induce triggered activity, and create spatial dispersion of refractoriness, resulting in a substrate for arrhythmias (2, 44). Calkins et al. (5) studied the sympathetic nervous system using the catecholamine analogue C-11 hydroxyephedrine (HED) and positron emission tomography (PET). They investigated the correlation between scintigraphic evidence of neuronal dysfunction and ventricular refractoriness in infarcted or cardiomyopathic human hearts with ventricular arrhythmia. They found that the effective refractory period in areas of myocardium demonstrating reduced C-11 HED retention was significantly longer

than in areas of myocardium demonstrating normal C-11 HED retention ($p < 0.001$). This suggests a relationship between abnormal sympathetic innervation and arrhythmogenesis in the structurally abnormal heart. Evidence also exists of heterogeneous innervation without structural abnormality (which is closely linked to fatal ventricular arrhythmias). Dae et al. (8) investigated cardiac sympathetic denervation using German shepherd dogs, with inherited spontaneous cardiac arrhythmias and associated sudden death, as a model of arrhythmogenic heart without structural abnormality. Upon I-123 MIBG imaging, they found 35 ± 16.5% of the left ventricle was denervated in the group of dogs with episodes of ventricular tachycardia (VT) and 12.0 ± 5.6% in groups without VT. Control dogs demonstrated significantly less denervation (4.0 ± 1.1%) than either of these two study groups. These findings suggest that the extent of heterogeneous innervation is related to the incidence of fatal arrhythmic episodes.

Cardiac sympathetic heterogeneity is also observed in patients with arrhythmogenic right ventricular cardiomyopathy (ARVC). ARVC is characterized by recurrent ventricular tachycardia, which frequently originated from the right ventricular outflow or inflow tract. The structural abnormality was also characterized by fibrolipomatous infiltration with degeneration of right ventricular myocardium that progress from the epicardium toward the endocardium, but left ventricular involvement is frequently observed. Wichter et al. (65) suggested that 40 of 48 ARVC patients (80%) demonstrated regional reductions or defects of I-123 MIBG uptake. The reduced tracer uptake was commonly involved in the basal posteroseptal region of the left ventricle, which was adjacent to the interventricular septum. The region is a common morphological substrate that is provided by the progressive degeneration of myocytes starting in the subepicardium and subsequent infiltration of fatty and fibrous tissue with interspersed surviving myocardial fibers.

Schaeffer et al. (50) reported on I-123 MIBG scintigraphy in patients with idiopathic left ventricular tachycardia (ILVT), idiopathic ventricular fibrillation (IVF) and right ventricular outflow tract tachycardia (RVO-VT). IVF and RVO-VT demonstrated a regional reduction in MIBG uptake, whereas ILVT patients demonstrated no such regional difference in MIBG uptake. The results of this study can be explained by the close relationship between the extent of heterogeneous innervation and the arrhythmic episodes.

It has been hypothesized that the long QT syndrome, which results in an increased incidence of ventricular arrhythmias, is the result of an imbalance of sympathetic cardiac innervation (28, 55, 56). However, recent studies using I-123 MIBG and C-11 HED, controversially suggest that heterogeneous sympathetic cardiac nervous function and distribution do not exist in long QT syndrome (6, 15, 32, 34). Furthermore, genetic analysis demonstrates that ion channel dysfunction is the primary defect in many forms of long QT syndrome which in turn triggers ventricular arrhythmia (43).

Brugada syndrome is characterized as a syndrome of right bundle branch block, right precordial ST-segment elevation and sudden death or syncope due to polymorphic ventricular tachycardia or ventricular fibrillation. Kasanuki et al. (21) found that increased vagal tone appears to be related to the initiation of ventricular fibrillation in patients without evidence of heart disease. In Brugada syndrome, studies using I-123 MIBG have demonstrated a variety of findings: almost normal regional uptake (29), inferioposterior reduced uptake (1, 37) and normal regional uptake with reduced global washout in the left ventricle (24). In view of these discrepant findings, the existence of sympathetic heterogeneous innervation in this disease is questioned.

Heterogeneity in other pathological conditions

Diseased human hearts, examined with I-123 MIBG or C-11 HED, were frequently found to have heterogeneous sympathetic innervation. Dilated cardiomyopathy (DCM) is frequently associated with regional neuronal dysfunction rather than with a perfusion abnormality (30). In DCM patients, the inferioposterior region is more commonly affected by neuronal dysfunction (67), and the heterogeneous innervation is linked to the severity or prognosis of the condition (16, 42, 64). Elevated plasma catecholamine levels result in competitive inhibition of presynaptic reuptake with global and/or regional reduction of the tracer uptake. This mechanism may partly explain the findings of impaired autonomic function in DCM patients.

Hypertrophic cardiomyopathy (HCM) is reported to involve sympathetic dysinnervation (27, 49). Studies revealed a global reduction in neuronal uptake of C-11 HED (49) and F-18 fluorodopamine (F-18 FDA) (27), which is also a tracer of catecholamines analogous to C-11 HED, in HCM patients compared to controls. In particular, Li et al. (27) focused on regional heterogeneity of sympathetic neuronal uptake in HCM, indicating that F-18 FDA retention corrected by perfusion was decreased in hypertrophied myocardial regions, but not in non-hypertrophied regions compared to myocardium in normal controls.

Systemic autonomic diseases frequently influence cardiac neuronal function (20, 39, 48). In particular, diabetes mellitus is often associated with autonomic neuropathy resulting in increased morbidity and mortality (13). Cardiac sympathetic neuronal dysfunction in patients with diabetes mellitus has been found using the

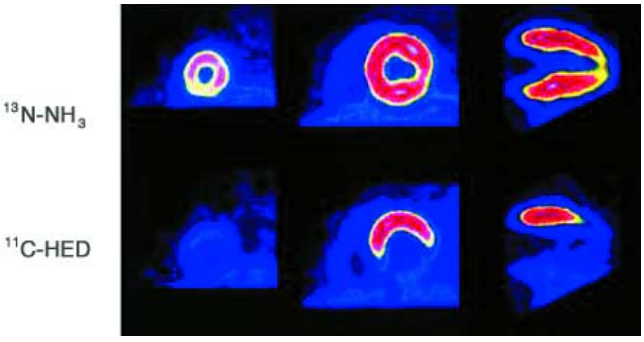

Fig. 2 PET images of the left ventricle in patients with diabetic autonomic neuropathy. Perfusion images using N-13 ammonia (top panels) are normal, whereas C-11 hydroxyephedrine (HED) retention is preserved only at the proximal segments of the left ventricle. The mismatch of perfusion and HED uptake identifies the area of sympathetic innervation.

above imaging methods (17, 26, 52, 63) even following negative clinical testing of the autonomic nervous system (52, 63). The imaging studies demonstrated a reduction in tracer uptake in the inferior wall of the left ventricle gradually spreading to adjacent segments. The extent of the reduced uptake was related to the severity of autonomic dysfunction as measured by conventional markers (17, 52).

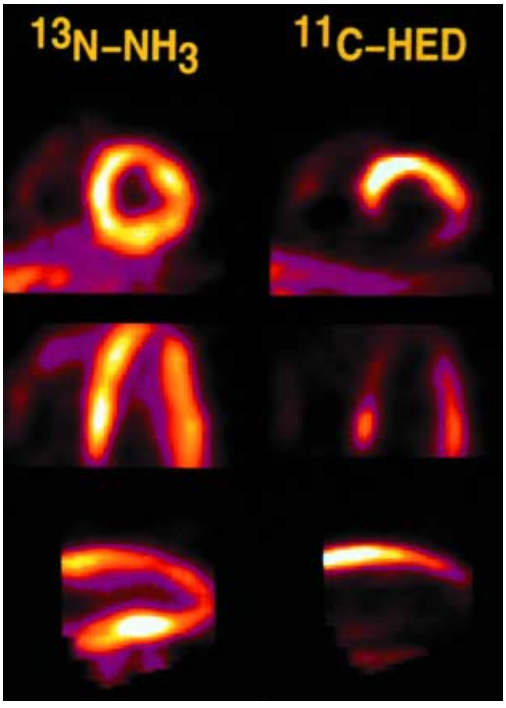

Fig. 3 PET images of the left ventricle in a patient 8 years after cardiac transplantation. Perfusion images (left) show homogeneous blood flow. C-11 HED images (right) indicate tracer retention in the anterior aspects of the left ventricle increasing from middle towards the base of the ventricle.

Stevens et al. (57) found, using C-11 HED PET, cardiac sympathetic denervation in the distal (apical) segments and inferioposterior regions of patients with diabetic neuropathy. In their study, rest myocardial blood flow in the distal denervated segments was greater in subjects with diabetic neuropathy than in diabetic subjects without neuropathy. Although the effects of sympathetic denervation on myocardial blood flow are not well understood, this finding may be explained by the fact that denervation induces myocardial capillary angiogenesis as found previously (61). Figure 2 shows an example of a C-11 HED PET image in a diabetic patient.

Parkinson's disease commonly presents with disturbances in autonomic function. In the heart, heterogeneous patterns of neuronal abnormalities, similar to those found in diabetes mellitus, have been reported (20). However the damage is actually heterogeneous and it is believed that this is because sympathetic nerves in the inferioposterior region are more easily damaged then elsewhere. In conditions such as aortic valve regurgitation, mitral valve regurgitation or aortic valve stenosis where pressure or volume overload of the heart occurs, abnormal heterogeneous sympathetic innervation has been found (45, 58). This innervation pattern is, once again, similar to that found in diabetes mellitus where I-123 MIBG imaging demonstrated a lower tracer uptake in the inferioposterior region: the extent of reduced uptake being correlated with the severity of disease (59).

Heterogeneous reinnervation following cardiac transplantation

As cardiac sympathetic fibers are severed during surgery, transplanted human hearts have demonstrated no localization of I-123 MIBG uptake shortly after transplantation (4, 7, 31, 54). However a number of studies report partial cardiac reinnervation at later time points after transplantation (4, 10, 11, 53). Using I-123 MIBG or C-11 HED, evidence was found of reinnervation primarily in the basal anterioseptal region and to a lesser degree in the inferioposterior and apical regions (4, 31, 53). Figure 3 shows an example of scintigraphic findings using C-11 HED PET.

The mid-ventricular region of the myocardium typically demonstrates less reinnervation than the basal region. Neurohormonal studies by Kaye et al. (22) have confirmed this observation. In their 1977 study on canine hearts, they found that norepinephrine concentrations recovered first in the left and right atrium followed by the basal left ventricular area; finally recovery was noted in the apical region two years after denervation. The findings of heterogeneous reinnervation can partly be explained by the fact that sympathetic neurons travel

along arterial structures, therefore, if reinnervation occurs, basal regions will be reached first by the newly grown fibers.

Conclusion

New imaging techniques, using tracer approaches, can visualize cardiac sympathetic innervation. Heterogeneity of tracer distribution, as a marker of variability in neuronal density and function, has been described in normal as well as diseased heart. The inferioposterior region shows typically less sympathetic innervation than the anterior region. In addition, neuropathic processes appear to commence in inferio-apical regions extending towards the base of the heart. Arrhythmogeneity has been related to the heterogeneous innervation of the heart and heterogeneous tracer uptake can be found in patients with arrhythmia. In dilated cardiomyopathy, reduced MIBG uptake indicates a poor prognosis which allows risk stratification for patients with heart failure to be calculated. Tracer approaches are uniquely suited to identify regionally altered innervation and provide tools for linking information on cardiac autonomic innervation with other clinical aspects.

References

1. Agostini D, Scanu P, Loiselet P, Babatasi G, Darlas Y, Grollier G, Potier JC, Bouvard G (1998) Iodine-123-metaiodobenzylguanidine SPECT of regional cardiac adrenergic denervation in Brugada syndrome. J Nucl Med 39: 1129–1132
2. Aidonidis I, Metz J, Gerstheimer F, Kubler W, Brachmann J (1993) Significance of cardiac innervation on spontaneous ventricular arrhythmias elicited by left stellate ganglion stimulation in dogs 4 days after myocardial infarction: comparison of two experimental models. Basic Res Cardiol 88: 155–166
3. Bengel F M, Barthel P, Matsunari I, Schmidt G, Schwaiger M (1999) Kinetics of 123I-MIBG after acute myocardial infarction and reperfusion therapy. J Nucl Med 40: 904–910
4. Bengel F M, Ueberfuhr P, Ziegler SI, Nekolla S, Reichart B, Schwaiger M (1999) Serial assessment of sympathetic reinnervation after orthotopic heart transplantation. A longitudinal study using PET and C-11 hydroxyephedrine. Circulation 99: 1866–1871
5. Calkins H, Allman K, Bolling S, Kirsch M, Wieland D, Morady F, Schwaiger M (1993) Correlation between scintigraphic evidence of regional sympathetic neuronal dysfunction and ventricular refractoriness in the human heart. Circulation 88: 172–179
6. Calkins H, Lehmann MH, Allman K, Wieland D, Schwaiger M (1993) Scintigraphic pattern of regional cardiac sympathetic innervation in patients with familial long QT syndrome using positron emission tomography. Circulation 87: 1616–1621
7. Dae M W, De Marco T, Botvinick EH, O'Connell J W, Hattner R S, Huberty JP, Yuen-Green MS (1992) Scintigraphic assessment of MIBG uptake in globally denervated human and canine hearts – implications for clinical studies. J Nucl Med 33: 1444–1450
8. Dae MW, Lee RJ, Ursell PC, Chin MC, Stillson CA, Moise NS (1997) Heterogeneous sympathetic innervation in German shepherd dogs with inherited ventricular arrhythmia and sudden cardiac death. Circulation 96: 1337–1342
9. Dae MW, O'Connell JW, Botvinick EH, Ahearn T, Yee E, Huberty JP, Mori H, Chin MC, Hattner RS, Herre JM et al. (1989) Scintigraphic assessment of regional cardiac adrenergic innervation. Circulation 79: 634–644
10. De Marco T, Dae M, Yuen-Green MS, Kumar S, Sudhir K, Keith F, Amidon TM, Rifkin C, Klinski C, Lau D et al. (1995) Iodine-123 metaiodobenzylguanidine scintigraphic assessment of the transplanted human heart: evidence for late reinnervation. J Am Coll Cardiol 25: 927–931
11. Estorch M, Camprecios M, Flotats A, Mari C, Berna L, Catafau AM, Ballester M, Narula J, Carrio I (1999) Sympathetic reinnervation of cardiac allografts evaluated by 123I-MIBG imaging. J Nucl Med 40: 911–916
12. Estorch M, Serra-Grima R, Flotats A, Mari C, Berna L, Catafau A, Martin JC, Tembl A, Narula J, Carrio I (2000) Myocardial sympathetic innervation in the athlete's sinus bradycardia: is there selective inferior myocardial wall denervation? J Nucl Cardiol 7: 354–358
13. Ewing DJ, Campbell IW, Clarke BF (1980) Assessment of cardiovascular effects in diabetic autonomic neuropathy and prognostic implications. Ann Intern Med 92: 308–311
14. Gill JS, Hunter GJ, Gane G, Camm AJ (1993) Heterogeneity of the human myocardial sympathetic innervation: in vivo demonstration by iodine 123-labeled meta-iodobenzylguanidine scintigraphy. Am Heart J 126: 390–398
15. Gohl K, Feistel H, Weikl A, Bachmann K, Wolf F (1991) Congenital myocardial sympathetic dysinnervation (CMSD) – a structural defect of idiopathic long QT syndrome. Pacing Clin Electrophysiol 14: 1544–1553
16. Hartmann F, Ziegler S, Nekolla S, Hadamitzky M, Seyfarth M, Richardt G, Schwaiger M (1999) Regional patterns of myocardial sympathetic denervation in dilated cardiomyopathy: an analysis using carbon-11 hydroxyephedrine and positron emission tomography. Heart 81: 262–270
17. Hattori N, Tamaki N, Hayashi T, Masuda I, Kudoh T, Tateno M, Tadamura E, Yonekura Y, Nakao K, Konishi J (1996) Regional abnormality of iodine-123-MIBG in diabetic hearts. J Nucl Med 37: 1985–1990
18. Imamura Y, Ando H, Mitsuoka W, Egashira S, Masaki H, Ashihara T, Fukuyama T (1995) Iodine-123 metaiodobenzylguanidine images reflect intense myocardial adrenergic nervous activity in congestive heart failure independent of underlying cause. J Am Coll Cardiol 26: 1594–1599
19. James RD, Christopher JB, Hopkins DA, Johnstone DE, Murphy DA, Armour JA (1986) Anatomy of human extrinsic cardio nerves and ganglia. Am J Cardiology 57: 299–309
20. Kanzaki N, Sato K, Hayabara T (1997) Improved cardiac iodine-123 metaiodobenzylguanidine accumulation after drug therapy in a patient with Parkinson's disease. Clin Nucl Med 22: 697–699

21. Kasanuki H, Ohnishi S, Ohtuka M, Matsuda N, Nirei T, Isogai R, Shoda M, Toyoshima Y, Hosoda S (1997) Idiopathic ventricular fibrillation induced with vagal activity in patients without obvious heart disease. Circulation 95: 2277–2285
22. Kaye MP, Randall WC, Hageman GR, Geis W P, Priola DV (1977) Chronology and mode of reinnervation of the surgically denervated canine heart: functional and chemical correlates. Am J Physiol 233: H431–437
23. Kobayashi H, Momose M, Kashikura K, Matsumoto N, Saito K, Asano R, Hosoda S, Kusakabe K (1995) Comparison of inferior myocardial defect between planar and SPECT image of ^{123}I-metaiodobenzylguanidine cardiac scintigraphy. Kaku Igaku 32: 205–209
24. Kobayashi H, Ohnishi S, Kusakabe K, Momose M, Matsuda N, Shoda M, Kasanuki H (1997) Decreased cardiac sympathetic activity in Brugada syndrome. Circulation 96: I-152 (abstract)
25. Kurata C, Wakabayashi Y, Shouda S, Okayama K, Yamamoto T, Ishikawa A, Suzuki K, Ishizuka T, Sakamoto S, Tawarahara K (1995) Enhanced cardiac clearance of iodine-123-MIBG in chronic renal failure. J Nucl Med 36: 2037–2043
26. Langer A, Freeman MR, Josse RG, Armstrong PW (1995) Metaiodobenzylguanidine imaging in diabetes mellitus: assessment of cardiac sympathetic denervation and its relation to autonomic dysfunction and silent myocardial ischemia. J Am Coll Cardiol 25: 610–618
27. Li ST, Tack CJ, Fananapazir L, Goldstein DS (2000) Myocardial perfusion and sympathetic innervation in patients with hypertrophic cardiomyopathy. J Am Coll Cardiol 35: 1867–1873
28. Miline JR, Ward DE, Spurrell RA, Camm AJ (1982) The long QT syndrome: effects of drugs and left stellate ganglion block. Am Heart J 104: 194–198
29. Miyazaki T, Mitamura H, Miyoshi S, Soejima K, Aizawa Y, Ogawa S (1996) Autonomic and antiarrhythmic drug modulation of ST segment elevation in patients with Brugada syndrome. J Am Coll Cardiol 27: 1061–1070
30. Momose M, Kobayashi H, Iguchi N, Matsuda N, Sakomura Y, Kasanuki H, Kusakabe K, Okawa T (1999) Comparison of parameters of ^{123}I-MIBG scintigraphy for predicting prognosis in patients with dilated cardiomyopathy. Nucl Med Commun 20: 529–535
31. Momose M, Kobayashi H, Ikegami H, Matsuda N, Hachida M, Kasanuki H, Kusakabe K (2000) Regional cardiac sympathetic reinnervation in transplanted human hearts detected by ^{123}I-MIBG SPECT imaging. Ann Nucl Med 14: 333–337
32. Momose M, Kobayashi H, Kasanuki H, Kusakabe K, Tamaki A, Onishi S, Okawa T (1998) Evaluation of regional cardiac sympathetic innervation in congenital long QT syndrome using ^{123}I-MIBG scintigraphy. Nucl Med Commun 19: 943–951
33. Morozumi T, Kusuoka H, Fukuchi K, Tani A, Uehara T, Matsuda S, Tsujimura E, Ito Y, Hori M, Kamada T, Nishimura T (1997) Myocardial iodine-123-metaiodobenzylguanidine images and autonomic nerve activity in normal subjects. J Nucl Med 38: 49–52
34. Muller KD, Jakob H, Neuzner J, Grebe SF, Schlepper M, Pitschner HF (1993) ^{123}I-metaiodobenzylguanidine scintigraphy in the detection of irregular regional sympathetic innervation in long QT syndrome. Eur Heart J 14: 316–325
35. Munch G, Nguyen NT, Nekolla S, Ziegler S, Muzik O, Chakraborty P, Wieland DM, Schwaiger M (2000) Evaluation of sympathetic nerve terminals with [^{11}C] epinephrine and [^{11}C] hydroxyephedrine and positron emission tomography. Circulation 101: 516–523
36. Napolitano LM, Willman VL, Hanlon CR, Cooper T (1965) Intrinsic innervation of the heart. Am J Physiol 208: 455–458
37. Nomura M, Nada T, Endo J, Kondo Y, Yukinaka M, Saito K, Ito S, Mori H, Nakaya Y, Shinomiya H (1998) Brugada syndrome associated with an autonomic disorder. Heart 80: 194–196
38. Nonidez JF (1939) Studies on the innervation of the heart. I. Distribution of cardiac nerves, with special reference to the identification of the sympathetic and parasympathetic preganglionics. Am J Anat 65: 361–413
39. Orimo S, Ozawa E, Nakade S, Sugimoto T, Mizusawa H (1999) ^{123}I -metaiodobenzylguanidine myocardial scintigraphy in Parkinson's disease. J Neurol Neurosurg Psychiatry 67: 189–194
40. Pace J B, Randall W C, Wechsler J S and Priola D V (1968) Alterations in ventricular dynamics induced by stimulation of the cervical vagosympathetic trunk. Am J Physiol 214: 1213–1218
41. Pierpont GL, DeMaster EG, Cohn JN (1984) Regional differences in adrenergic function within the left ventricle. Am J Physiol 246: H824–829
42. Pietila M, Malminiemi K, Ukkonen H, Saraste M, Nagren K, Lehikoinen P, Voipio-Pulkki LM (2001) Reduced myocardial carbon-11 hydroxyephedrine retention is associated with poor prognosis in chronic heart failure. Eur J Nucl Med 28: 373–376
43. Priori SG, Barhanin J, Hauer RN, Haverkamp W, Jongsma HJ, Kleber AG, McKenna WJ, Roden DM, Rudy Y, Schwartz K, Schwartz PJ, Towbin JA, Wilde AM (1999) Genetic and molecular basis of cardiac arrhythmias: impact on clinical management parts I and II. Circulation 99: 518–528
44. Priori SG, Corr PB (1990) Mechanisms underlying early and delayed afterdepolarizations induced by catecholamines. Am J Physiol 258: H1796–1805
45. Rabinovitch MA, Rose CP, Schwab AJ, Fitchett DH, Honos GN, Stewart JA, Chen LF, Castilla EP, Gomez AA, Abrahamowicz M (1993) A method of dynamic analysis of iodine-123-metaiodobenzylguanidine scintigrams in cardiac mechanical overload hypertrophy and failure. J Nucl Med 34: 589–600
46. Randall WC, Szentivanyi M, Pace JB, Wechsler JS, Kaye MP (1968) Patterns of sympathetic nerve projections onto the canine heart. Circ Res 22: 315–323
47. Sakata K, Shirotani M, Yoshida H, Kurata C (1998) Physiological fluctuation of the human left ventricle sympathetic nervous system assessed by iodine-123-MIBG. J Nucl Med 39: 1667–1671
48. Satoh A, Serita T, Seto M, Tomita I, Satoh H, Iwanaga K, Takashima H, Tsujihata M (1999) Loss of ^{123}I-MIBG uptake by the heart in Parkinson's disease: assessment of cardiac sympathetic denervation and diagnostic value. J Nucl Med 40: 371–375
49. Schafers M, Dutka D, Rhodes CG, Lammertsma AA, Hermansen F, Schober O, Camici PG (1998) Myocardial presynaptic and postsynaptic autonomic dysfunction in hypertrophic cardiomyopathy. Circ Res 82: 57–62
50. Schafers M, Wichter T, Lerch H, Matheja P, Kuwert T, Schafers K, Borggrefe M, Breithardt G, Schober O (1999) Cardiac ^{123}I-MIBG uptake in idiopathic ventricular tachycardia and fibrillation. J Nucl Med 40: 1–5
51. Schlack W, Schafer S, Thämer V (1994) Left stellate ganglion block impairs left ventricular function. Anesth Analg 79: 1082–1088
52. Schnell O, Muhr D, Weiss M, Dresel S, Haslbeck M, Standl E (1996) Reduced myocardial ^{123}I-metaiodobenzylguanidine uptake in newly diagnosed IDDM patients. Diabetes 45: 801–805
53. Schwaiger M, Hutchins GD, Kalff V, Rosenspire K, Haka MS, Mallette S, Deeb GM, Abrams GD, Wieland D (1991) Evidence for regional catecholamine uptake and storage sites in the transplanted human heart by positron emission tomography. J Clin Invest 87: 1681–1690
54. Schwaiger M, Kalff V, Rosenspire K, Haka MS, Molina E, Hutchins GD, Deeb M, Wolfe E Jr, Wieland DM (1990) Noninvasive evaluation of sympathetic nervous system in human heart by positron emission tomography. Circulation 82: 457–464
55. Schwartz P, E.H L, Moss AJ, Crampton RS, Trazzi R, Ruberti U (1991) Left cardiac sympathetic denervation in the therapy of congenital long QT syndrome – Worldwide report. Circulation 84: 503–511

▶

56. Schwartz P, Periti M, Mallini A (1975) Fundamentals of clinical cardiology. Am Heart J 89: 378–390
57. Stevens MJ, Dayanikli F, Raffel DM, Allman KC, Sandford T, Feldman EL, Wieland DM, Corbett J, Schwaiger M (1998) Scintigraphic assessment of regionalized defects in myocardial sympathetic innervation and blood flow regulation in diabetic patients with autonomic neuropathy. Journal of the American College of Cardiology 31: 1575–1584
58. Terada K, Sugihara H, Shiga K, Ohtsuki K, Ito K, Taniguchi Y, Azuma A, Kohno Y, Miyao K, Nakagawa M (1995) Clinical evaluation of ^{123}I-metaiodobenzylguanidine myocardial scintigram in patients with valvular heart disease. J Cardiol 25: 247–253
59. Terada K, Sugihara H, Tatsukawa H, Keira N, Morimoto S, Inoue K, Katoh S, Nakagawa M (1997) Angle of defect on ^{123}I-MIBG myocardial SPECT. Kaku Igaku 34: 113–117
60. Thames MD, Klopfenstein HS, Abboud FM, Mark AL, Walker JL (1978) Preferential distribution of inhibitory cardiac receptors with vagal afferents to the inferoposterior wall of the left ventricle activated during coronary occlusion in the dog. Circ Res 43: 512–519
61. Tomanek R (1989) Sympathetic nerves modify mitochondrial and capillary growth in normotensive and hypertensive rats. J Moll Cell Cardiol 21: 755–764
62. Tsuchimochi S, Tamaki N, Tadamura E, Kawamoto M, Fujita T, Yonekura Y, Konishi J (1995) Age and gender differences in normal myocardial adrenergic neuronal function evaluated by iodine-123-MIBG imaging. J Nucl Med 36: 969–974
63. Turpeinen AK, Vanninen E, Kuikka JT, Uusitupa MI (1996) Demonstration of regional sympathetic denervation of the heart in diabetes. Comparison between patients with NIDDM and IDDM. Diabetes Care 19: 1083–1090
64. Vesalainen RK, Pietila M, Tahvanainen KU, Jartti T, Teras M, Nagren K, Lehikoinen P, Huupponen R, Ukkonen H, Saraste M, Knuuti J, Voipio-Pulkki LM (1999) Cardiac positron emission tomography imaging with [^{11}C]-hydroxyephedrine, a specific tracer for sympathetic nerve endings, and its functional correlates in congestive heart failure. Am J Cardiol 84: 568–574
65. Wichter T, Hindricks G, Lerch H, Bartenstein P, Borggrefe M, Schober O, Breithardt G (1994) Regional myocardial sympathetic dysinnervation in arrhythmogenic right ventricular cardiomyopathy. An analysis using ^{123}I-meta- iodobenzylguanidine scintigraphy. Circulation 89: 667–683
66. Wieland D, Brown L, Rogers W, Worthington K, Wu J, Clinthorne N (1981) Myocardial imaging with a radioiodinate norepinephrine storage analogue. J Nucl Med 22: 22–31
67. Yamazaki J, Muto H, Ishiguro S, Okamoto K, Hosoi H, Nakano H, Morishita T (1997) Quantitative scintigraphic analysis of ^{123}I-MIBG by polar map in patients with dilated cardiomyopathy. Nucl Med Commun 18: 219–229
68. Zipes DP, Barber J, Takahashi N, Gilmour RF (1983) Influence of the autonomic nervous system on the genesis of cardiac arrhythmias. Pacing Clin Electrophysiol 6: 1210–1220